Journal of the Argentine Chemical Society

CHARACTERIZATION OF VO_x/ZrO_2 CATALYSTS AND THEIR ACTIVITY IN THE OXIDATION OF CARBON MONOXIDE

Delia Gazzoli[a]*, Sergio De Rossi[b], Giovanni Ferraris[b] and Mario Valigi[a]

[a]*Dipartimento di Chimica, Sapienza Università di Roma, P.le A. Moro, 5, I-00185 Rome, Italy*

[b]*Consiglio Nazionale delle Ricerche, Istituto dei Sistemi Complessi, ISC, UOS "Materiali Inorganici e Catalisi Eterogenea" (MICE), c/o Dipartimento di Chimica, Sapienza Università di Roma, P.le A. Moro, 5, I-00185 Rome, Italy*

***E-mail:** delia.gazzoli@uniroma1.it*

Phone: 39-06-49913377. Fax: 39-06-490324

Received December 23, 2008. In final form March 12, 2009.

Abstract

Zirconia-supported vanadium oxide samples, prepared by equilibrium adsorption method in acid (pH 2.7) and basic (pH 10) conditions using hydrous zirconium oxide, ZrO_2(383), and heated at 823 K for 5 h in air, were characterized by X-ray diffraction, "in situ" Raman spectroscopy, temperature programmed reduction and tested for the CO oxidation reaction. Depending on vanadium loading, various VO_x species formed either in a disperse form predominately as polyvanadate species on the zirconia surface or as separate phases (ZrV_2O_7, V_2O_5) or both. Leaching treatments with ammonia revealed that only a fraction of the dispersed species interacts directly with the support surface and disclosed the presence of ZrV_2O_7 already in the most dilute sample. The activity of unsupported V_2O_5 and ZrV_2O_7 for the oxidation of CO, in a flow microreactor and in the temperature range 373 – 602 K, was in the order: $V_2O_5 < ZrV_2O_7$. On

VO_x/ZrO_2 catalysts the activity increased with V loading up to a constant value, indicating a surface fully covered by VO_x species. On leached samples both apparent activation energy and pre-exponential factor increased, suggesting a role of both interacting VO_x and ZrV_2O_7 species.

Keywords: CO oxidation, V_2O_5/ZrO_2, Zirconia, Raman spectroscopy, TPR.

Resumen

Muestras de óxido de Vanadio soportado sobre zirconia, preparadas por el método de equilibrio de adsorción en condiciones ácidas (pH 2.7) y básicas (pH 10) usando óxido de zirconio, ZrO_2(383), calentado a 823 K por 5 h en aire se caracterizaron por difracción de rayos X, espectroscopía Raman "in situ", reducción programada de temperatura y se probaron para la reacción de oxidación del CO. Dependiendo de la carga de Vanadio, se formaron varias especies VO_x ya sea de una forma dispersa predominantemente como especies de polivanadato sobre la superficie de zirconio o como fases separadas o ambas. El tratamiento con amoníaco revela que solo una fracción de las especies dispersas interactúa directamente con la superficie el soporte mostrando la presencia de ZrV_2O_7 aún en la muestra mas diluida. La actividad del V_2O_5 y del ZrV_2O_7 no soportados para la oxidación del CO. En un microrreactor de flujo y en un rango de temperatura de 373 – 602 K, estuvo en el orden $V_2O_5 < ZrV_2O_7$, Sobre el catalizador VO_x/ZrO_2, la actividad aumenta con la carga de V hasta un valor constante indicando una superficie totalmente cubierta por especies VO_x. Sobre las muestras tratadas la energía de activación aparente y el factor pre-exponencial aumentan sugiriendo un rol de ambas especies interactuantes VO_x y ZrV_2O_7.

Palabras clave: oxidación de CO, V_2O_5/ZrO_2, Zirconia, epectroscopía Raman, TPR.

Introduction

Vanadium (V) oxide is an active material for several important catalytic reactions, especially oxidation reactions [1-6]. As alone, however, V_2O_5 can not maintain a high surface area in reaction conditions and spreading it on a suitable high surface area support is employed to hinder thermal sintering. Among the others, alumina, ceria, titania and zirconia have been investigated as supports for vanadia [7-9]. The redox properties of vanadia-based mixed oxides have very recently been investigated by Shah et. al. [10]. On the other hand, vanadium oxides are quite reactive materials and in some instances solid solutions or even compounds can result from the vanadium oxides species and support interaction. This interaction influences the properties of both the VO_x surface species (es. nuclearity, and redox properties) and the support (es. phase transitions and surface area).

In the last few years, we investigated the VO_x/ZrO_2 system in great detail in that concerns solid state, surface chemistry and morphology [11, 12, 13]. We also recently investigated the activity and selectivity in n-butane oxidative dehydrogenation and their correlation with VO_x surface species [14]. To gain further information on the relation between surface composition and catalytic activity in a somehow easier reaction, we have undertaken a study of CO oxidation, a reaction that in the past was investigated by Rozeboom et al. [7] and Mori et al. [8]. They concluded that the reaction takes place with a reduction/oxidation mechanism, with reduction as the rate determining step.

Preliminary results on CO oxidation deserving attention are presented in this paper together with a careful characterization of VO_x/ZrO_2 samples by several techniques, including X-ray diffraction, "in situ" Raman spectroscopy and temperature programmed reduction.

Experimental

Samples preparation and chemical analysis.

Hydrous zirconium oxide, hereafter designated as $ZrO_2(383)$, was obtained by precipitation with a stream of ammonia-saturated N_2 from a $ZrOCl_2$ solution and dried at 383 K in air for 24 h, as already reported [15]. The vanadium-containing samples were obtained by suspending an amount of $ZrO_2(383)$ in a relatively large volume of V(v) aqueous solution (from NH_4VO_3, Fluka) at a given pH (10 or 2.7) fixed by NH_4OH or HNO_3. The suspension was shaken for 72 h at room temperature to equilibrate the system. The solid was filtered from the liquid fraction, dried at 383 K for 24 h and finally heated in air at 823 K, 5 h. The samples were designated as ZVx,y where x stands for the vanadium content as wt.% (metal) and y the pH value (Table 1). Two fractions of $ZrO_2(383)$, submitted to similar procedures (contact with vanadium-free aqueous solutions at pH 10 or 2.7, shaking, filtering, heating at 823 K), yielded solids with similar properties hereafter indicated as $ZrO_2(823)$.

V_2O_5 was obtained by decomposing NH_4VO_3 (Fluka) in air at 873 K for 3 h. ZrV_2O_7 was prepared from a mixture of V_2O_5 and $ZrO_2(383)$ heated in air at 983 K following the procedure described by Sanati et al.[16].

Because V_2O_5 is soluble in ammonia solution [17], a portion of each sample (typically 70 mg) was contacted with a hot ammonia solution (about 20 mL, 2 $mol \cdot L^{-1}$) in a closed vessel for 30 minute, under stirring. The solid was then separated and leached three times. The liquid fractions were collected and the vanadium content was determined by atomic absorption (see below). ZrV_2O_7 washed in similar manner released no detectable vanadium. Leached samples were designated as ZVx,yLz, where L stands for leached and z is the vanadium concentration in the sample after leaching.

The vanadium content was determined by atomic absorption after dissolving the sample in a concentrated HF solution, and subsequent dilution, as already reported [18]. The V standard solution (Fluka 1000 ppm) contained ZrO_2, dissolved in HF, in a concentration similar to that of the samples.

Experimental methods.

X-ray diffraction (XRD) patterns in the 2θ angular range from 5 to 60° were obtained by a Philips PW 1729/10 diffractometer and Cu Kα (Ni-filtered) radiation.

Surface area measurements (BET method) were performed by N_2 adsorption at 77 K using a ASAP 2010 Micromeritics apparatus on samples outgassed under vacuum for 2 h at 473 K, before the measurement.

Raman spectra were collected with a SPECS triple spectrograph, in macro configuration, equipped with a liquid-nitrogen-cooled CCD detector using the 514.5 nm line of an Ar^+ laser. The laser power on the sample was always kept under 20 mW. The spectral resolution was 1.4 cm^{-1}. The samples were pressed into 5 mm pellets and analyzed in air or using a *in situ* cell [19]. In the *in situ* experiment, the sample was heated in flowing dry oxygen at 673 K, 2 h and the spectra were collected after cooling to 298 K always in dry oxygen. Raman spectra analysis was performed by a GRAMS/386 software by Galactic.

Temperature-programmed reduction (TPR) was measured in a flow system using a HWD detector and a gas mixture containing 10 vol% of hydrogen in nitrogen 1.8 dm^3/h, heating rate 8 K/min. The gases were dried and purified with suitable filters and their flows regulated with Brooks electronic mass flow controllers. For the measurement, 60 mg of sample, located in a tubular reactor, underwent oxidative pre-treatment in a flow of oxygen (20 vol%) in nitrogen at 723 K, 1 h, were cooled to room temperature in a nitrogen flow and then equilibrated in the reaction mixture.

The catalytic activity measurements were carried out in a flow microreactor previously described [20]. The catalyst (0.2 – 0.5 g, powder) was pretreated in a flow (50 mL NTP min^{-1}) of dry oxygen at 673 K for 30 min. After cooling at 373 K, the reactant mixture ($CO:O_2$:He 0.5:20:79.5 molar) was admitted to the reactor at a space velocity of 30000 mL NTP h^{-1} g_{cat}^{-1}. At the same time a linear temperature ramp of 1 K min^{-1} from 373 to 603 K was started, with GC analysis of reactants and product every 10 min (10 K). The analysis was performed with a Carlo Erba 6000 Vega Series 2 gas-chromatograph using a CTR1 column from Alltech and a thermal conductivity detector. Peak integration was accomplished with software IQ3 from DANI. Reported velocity constants, k (s^{-1} m^{-2}), were calculated from CO to CO_2 conversions applying 1st order kinetics with respect to CO and normalizing for the exposed area of the catalyst.

Results and Discussion

Structural characterization

Previous studies on zirconia-supported vanadium systems, prepared by equilibrium adsorption using hydrous zirconium oxide as starting material [11, 12, 14], disclosed that the spreading of vanadium species depended on the preparation conditions (pH 10 and pH 2.7) and on vanadium loading. In addition, a treatment with an ammonia solution, able to dissolve V_2O_5 and vanadia-like amorphous polymers, indicated that the two sets of samples differed in the amount of vanadium strongly interacting with the zirconia surface [12]. This treatment can give an estimate of the amount of vanadium species strongly anchored on the zirconia surface that affected some support properties, such as sintering and phase transition [11, 12].

It must be recalled that, using the equilibrium adsorption method, the molecular structures of the supported species are determined not only by the point of zero charge of the support (PZC) and the pH of the impregnating solution, but also by the porous structure of the support. Hydrous zirconium oxide possesses micropores and narrow mesopores and has a PZC of about 6.7 [21, 22]. In aqueous solution the structure of the anionic vanadium species depends both on pH and on solution concentration. In the vanadium concentration range used in the present study, at pH 2.7 the large $H_zV_{10}O_{28}^{(6-z)-}$ (where z may be 0, 1 or 2) anions are predominant, while at pH 10 the most abundant species are the small $V_2O_7^{4-}$ entities [23, 24]. It has been shown that the presence of micropores hinders the uptake of large polyanions which suffer diffusion limitations [25].

The characterization of thermally treated samples at 823 K in air for 5 h showed that, depending on vanadium loading, several vanadium species formed. At low vanadium content (x<2%) both series of samples contained highly dispersed vanadium species. For higher loadings, comparing samples with similar concentration, the vanadium fraction in a dispersed state was higher in samples at pH 10 than in those prepared at pH 2.7, as indicated by the absence in the XRD patterns of ZVx,10 samples of lines other than those of monoclinic and tetragonal ZrO_2, Table 1. By contrast the presence in the XRD spectra of ZVx,2.7 samples with x > 4.5 wt% of lines of ZrV_2O_7 or V_2O_5 or both confirms the presence of vanadium crystalline species.

Raman spectroscopy under dehydrated conditions ("in situ" treatment at 673 K, 2h in flowing dry oxygen) was applied to determine the structure of the supported vanadia species. It is well documented that hydration affects vanadium surface species probably via hydrogen bonding resulting in a shift to lower frequencies and broadening of the terminal V=O band [26].

The Raman spectra, illustrated for some typical ZVx,2.7 and ZVx,10 samples, were characterized by bands in the range 200-700 cm^{-1} due to ZrO_2 (monoclinic and tetragonal) and by a composite feature spanning the frequencies range 750-1030 cm^{-1} due to vanadium species, Fig. 1 and 2. At increasing vanadium content the bands of ZrO_2 progressively diminished in intensity and in the ZV7.40,2.7 sample they were barely detectable (Fig.1 B, curve a'), as it might be expected for the deposition of species forming progressively larger and thick structures. At low vanadium

loading the spectra are characterized by a weak band at about 1020 cm^{-1} and a broad feature lying between 750 and 900 cm^{-1} (Fig. 1A curve a). The first band, characteristic of V=O stretching vibrations within isolated monovanadate [26-28] or terminal V=O bond of polymeric species [29], appeared to shift to higher frequencies with increasing vanadia loading, (Fig. 1B, curve a'; Fig.2A, curves a and 2B, curves a'). The feature in the range 750-900 cm^{-1}, corresponding to V-O-V vibrations in polyvanadate structures, became progressively more complex with the appearance of bands at 775 cm^{-1} and 989 cm^{-1} revealing the formation of ZrV_2O_7, and at 998 cm^{-1} identifying the presence of V_2O_5 (Fig. 1B, curve a').

In the spectra for leached samples ZrO_2 bands typically increased in intensity, the broad feature in the region 800-950 cm^{-1} decreased and the components that in the samples before leaching appeared at $\nu > 1015$ cm^{-1} disappeared (Fig. 1 and 2). These changes, barely detectable in the ZV1.2 sample (Fig. 1A, curve b), were more pronounced at high vanadium loading (Fig. 1B, curve b'; Fig. 2A, curve b and Fig. 2B curve b'). The reduced intensity of the broad feature at about 800-950 cm^{-1} disclosed a significant contribution of a band at about 776 cm^{-1} (due to ZrV_2O_7) in all the samples, eventually becoming the strongest feature in the ZV7.4,2.7 sample (Fig. 1B, curve b').

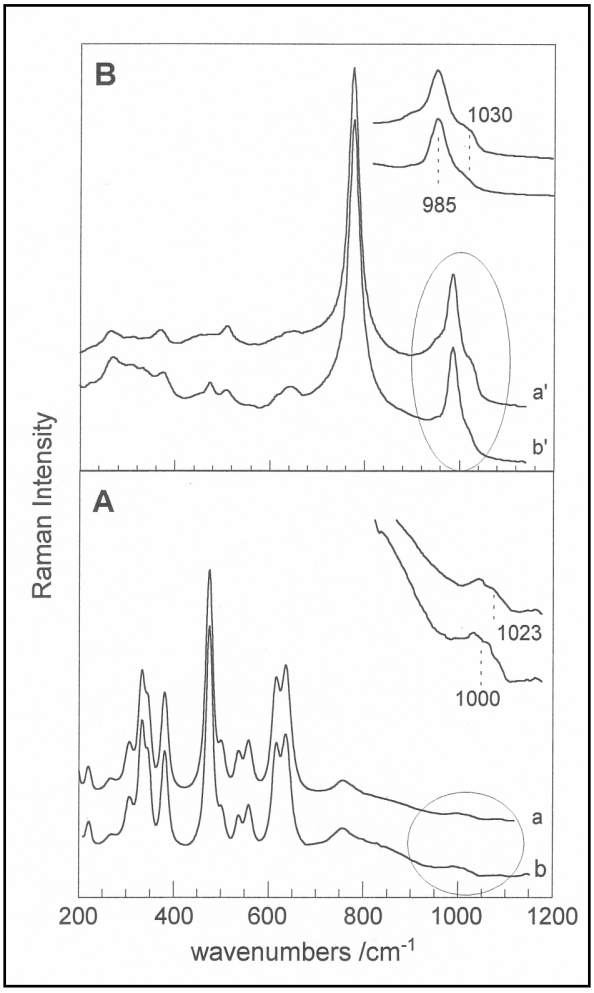

Figure 1.Raman spectra after *in situ* treatments.
Section A: curve a, ZV1.2,2.7; curve b, ZV1.2,2.7L1.1;
Section B: curve a', ZV7.4,2.7; curve b', ZV7.4,2.7L5.8

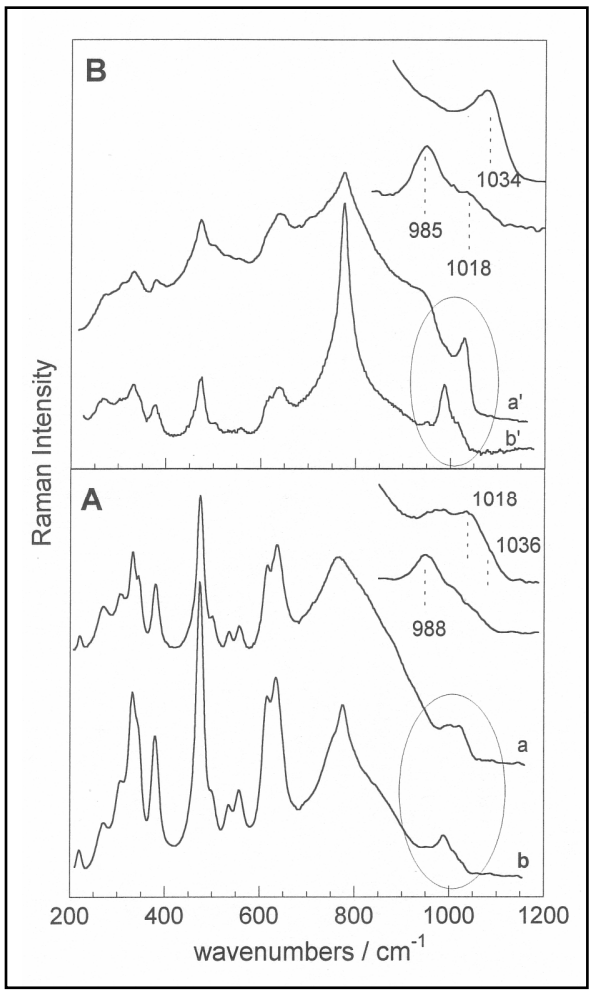

Figure 2. Raman spectra after *in situ* treatments.
Section A: curve a, ZV2.7,10; curve b, ZV2.7,10L1.4;
Section B: curve a', ZV5.4,10; curve b', ZV5.4,10L3.0

Changes in the surface morphology of zirconia-supported vanadium oxide systems with ammonia leaching were directly imaged by atomic force microscopy (TM-AFM) [13]. It was found that the leaching treatment removed almost completely the large structures grown layered and some aggregates became more clearly visible.

We assigned the progressive shift to higher frequency of the bands in the range 1000-1030 cm^{-1} and the concomitant growing intensity of the broad feature in the region 750-950 cm^{-1} to the presence of polyvanadate structures that increase in size or numbers or both with increasing surface vanadium density. Even in the more dilute sample, Fig. 1A, curve a, the band at about 1010 cm^{-1}, occurring with the broad feature at about 850 cm^{-1}, suggests polyvanadate structures although monovanadate species may contribute. Monomeric VO_4 species on different supports including ZrO_2 have been reported in a recent paper for samples with loading well below 1 V atoms nm^{-2} [30].

The vanadium species remaining on the zirconia surface after ammonia leaching are still polyvanadate structures with a lower condensation degree, the band due to V=O stretching (about 1015 cm^{-1}) being accompanied by the related feature at 850 cm^{-1} (V-O-V modes) in all the ZVxL samples, and ZrV_2O_7 entities. Furthermore, already in the more dilute sample, leaching disclosed a band at about 770 cm^{-1} (Fig. 1A, curve b) assigned to ZrV_2O_7-like structures.

The coexistence of vanadium species in various molecular configuration on the zirconia surface was also revealed by TPR analysis.

By comparing the TPR curves of some ZVx,10 and ZVx2.7 samples in Fig. 3 and Fig. 4, it can be concluded that the increase in V loading affects the shape of the reduction peaks and the temperature of the peak maximum. TPR envelops resulted from the superimposition of a strong component at about 713 K and from H_2 uptakes at lower (523-623 K) and higher (773-923) temperatures (Fig. 3A, curve a). At increasing vanadium content the main peak increased in intensity (Fig. 3 B, curve a') and progressively shifted to the 770-820 K range (Fig. 4B, curve a'), the temperature range at which ZrV_2O_7 reduces [31]. In ZVx,2.7 samples with vanadium content higher than x>7.4 wt% a peak at about 900 K identified V_2O_5 (figure not shown). The removal of large polymeric species (V_2O_5-like) and V_2O_5 crystallites by leaching treatments yielded simplified TPR profiles. The H_2 consumption strongly decreased in the range 600-800 K for both sets of samples (Fig. 3 A, curve b and 3 B, curve b'; Fig. 4A curve b and 4B, curve b'). The main component shifted towards higher temperature at increasing vanadium content: from about 600 K for the most dilute sample (ZV1.2,2.7L1.1), Fig. 4A curve b, to about 800 K for the most concentrated sample (ZV7.4,2.7L5.8), Fig. 4A, curve b. Although it is difficult to differentiate the peaks in the TPR profiles as reduction of specific vanadium species, on the basis of previous findings [13], the reduction profile of the leached samples can be considered as the convolution of at least three vanadium species: small polymeric VO_x entities anchored to the zirconia surface (hydrogen consumption in the range 580-620 K), large polymeric structures (in the range 680-730 K) and ZrV_2O_7 or ZrV_2O_7-like aggregates (in the range 770-820 K). According to literature data [32, 33], the small polymeric species are reported to reduce faster and at temperatures lower than both monovanadate and large polymeric structures, confirming the reducibility sequence proposed by Deo and Wachs [34]: V-O-V > V-O-$(V)_2$ > V=O. Therefore, in agreement with the Raman conclusion, the TPR data confirm the presence of polymeric vanadium species in our samples. As the concentration increases, the vanadium polymeric structures grow, ZrV_2O_7 forms and the reduction shifts to higher temperature.

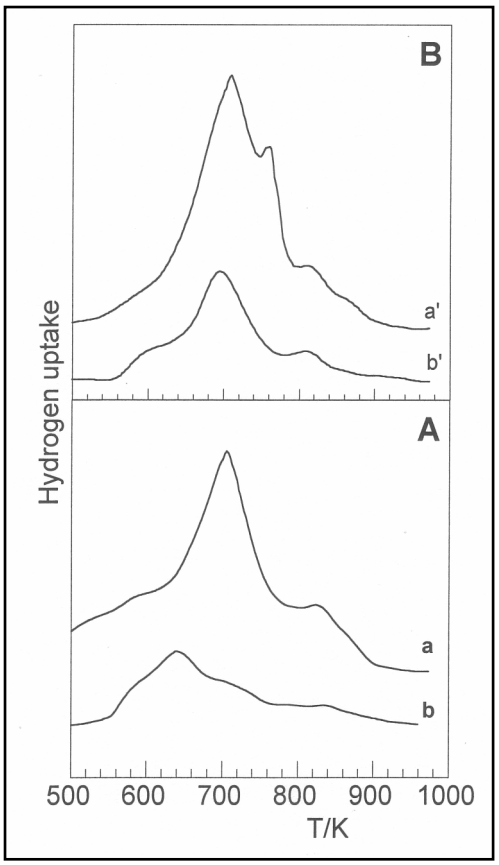

Figure 3. TPR profiles of some representative ZV*x*,10 samples before and after leaching. Section A: a - ZV2.7,10; b - ZV2.7,10L1.4. Section B: a' - ZV5.4,10; b' - V5.4,10L3.0.

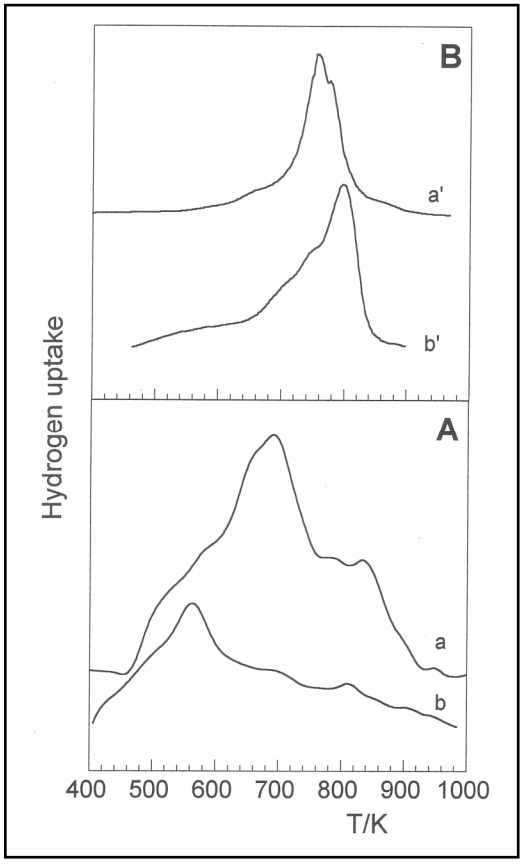

Figure 4. TPR profiles of some representative ZV*x*,2.7 samples before and after leaching. Section A: a - ZV1.2,2.7; b- ZV1.2,2.7L1.1. Section B: a' - ZV7.4,2.7; b' - ZV7.4,2.7L5.8

Catalytic oxidation of carbon monoxide

The activity of the reference compounds increased in steps of two order of magnitude in the sequence: $ZrO_2 < V_2O_5 < ZrV_2O_7$ in the explored range of temperature (from 373 to 603 K), Fig.5. The values of their pre-exponential factor, k_o, span from 90 s^{-1} m^{-2} (ZrO_2) to 190 s^{-1} m^{-2} (V_2O_5), Table 1, indicating that the differences in activity should chiefly depend on the differences in the apparent activation energy, Ea, values. Roozeboom et al. [7] showed that V_2O_5 exhibits different value of Ea depending on preparation history. For well stabilized V_2O_5 Ea ~107 kJ mol^{-1} was measured, whilst it was ~80 kJ mol^{-1} for V_2O_5 freshly decomposed from NH_4VO_3 (600 K, 2 h). The Ea value measured in this study, ~ 92 k $Jmol^{-1}$, is in agreement with the previous results, taking into account that V_2O_5 was decomposed from NH_4VO_3 at 873 K for 3 h.

V_2O_5 contains V-O-V bridges, ZrV_2O_7 exhibits both Zr-O-V and V-O-V bonds [35]. Comparing the V_2O_5 and ZrV_2O_7 activities, the higher value exhibited by ZrV_2O_7 suggests an important role of the Zr-O-V sites. As for reducibility, ZrV_2O_7 reduced more easily than V_2O_5 [7].

Despite the careful characterization of our ZVx,y samples, we were not able to quantify the fraction of vanadium present in the different molecular structures. Therefore, for simplicity, we restrict the analysis of the catalytic data to dilute ZVx,y ($x \leq 2.4$) and concentrated ZVx,2.7 ($x \geq 7.4$) samples for which the predominant vanadium species are more clearly established.

The apparent activation energy values of the as prepared ZVx,y catalyst range from 66.9 and 79.4 kJ mol^{-1}. The level of activity of ZVx,y catalysts substantially increases with V content up to the sample ZV7.4,2.7. A further increase of V loading leaves the activity unchanged (sample ZV22.2,2.7), Fig. 6. These findings can be explained taking into account that in dilute samples (ZV1.2,2.7 and ZV2.7.10) the majority of polyvanadate species are spread on the surface as small entities (Raman and TPR evidences) and are all accessible to the reactants. At increasing V loadings polyvanadate species increase in size or number or both, eventually covering all the support surface, yielding almost constant surface composition.

Table 1. Main characteristics (Specific surface area, *S*; surface concentration; crystalline phases) and CO oxidation results (pre-esponential factor, k_o, apparent activation energy, E_a for ZVx,y e ZVx,yLz. samples.

Samples[(a)]	S/m^2g^{-1}	Phase[(b)]	$k_o/s^{-1}m^{-2}$	$E_a/kJmol^{-1}$
ZrO_2(823)	48	m, t	$9.0\ 10^1$	100
V_2O_5	4.8	V	$1.9\ 10^2$	92
ZrV_2O_7	2.9	Z	$1.2\ 10^2$	75
ZV1.2,2.7	60	m, t	4.2	79
ZV2.7,10	77	m, t	4.0	75
ZV7.4,2.7	24	m, t, Z, V	1.1	67
ZV22.2,2.7	21	m, t, Z, V	$2.0\ 10^1$	79
ZV1.2,2.7L1.1	60	m, t	$2.8 \cdot 10^4$	117
ZV2.7,10L1.4	78	m, t	$5.0 \cdot 10^5$	125
ZV22.2,2.7L7.9	37	m, t, Z	$5.9 \cdot 10^{10}$	163

[(a)] For sample designation, see text.
[(b)] m=ZrO_2 monoclinic; t=ZrO_2 tetragonal; Z= ZrV_2O_7; V= V_2O_5

The ammonia-leached samples, Fig. 7, displayed considerably higher apparent activation energy (from 117 kJ mol^{-1}, ZV1.2,2.7L1.1, to 163 kJ mol^{-1}, ZV22.2,2.7L7.9), suggesting that the active sites are different and less efficient than those present on the as prepared samples. This holds in the approximation that the heats of adsorption do not change significantly so that their effects on the apparent activation energy values are comparable. Compared to the as prepared samples, the leached samples had much higher k_0 values, Table 1.

In a heterogeneously catalyzed reactions, k_o depends both on activation entropy and number of active sites because the frequency of collisions with the active sites is proportional to their number. As a change of many order of magnitude in the number of active sites is hardly conceivable ($5.9 \cdot 10^{10}/2.8 \cdot 10^4 = 2 \cdot 10^6$), we suggest that the entropic term of k_0 is the one that varies to a larger extent.

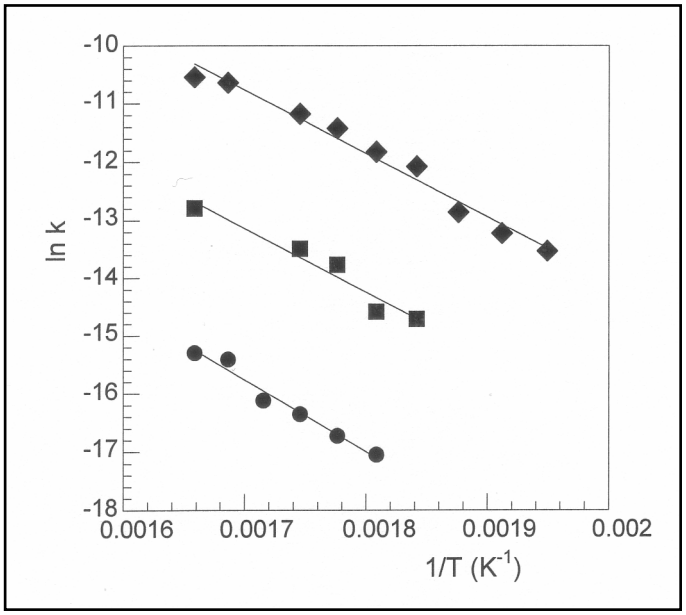

Figure 5. Arrhenius plots of CO oxidation for reference compounds:
●- ZrO_2; ■- V_2O_5; ◆- ZrV_2O_7.

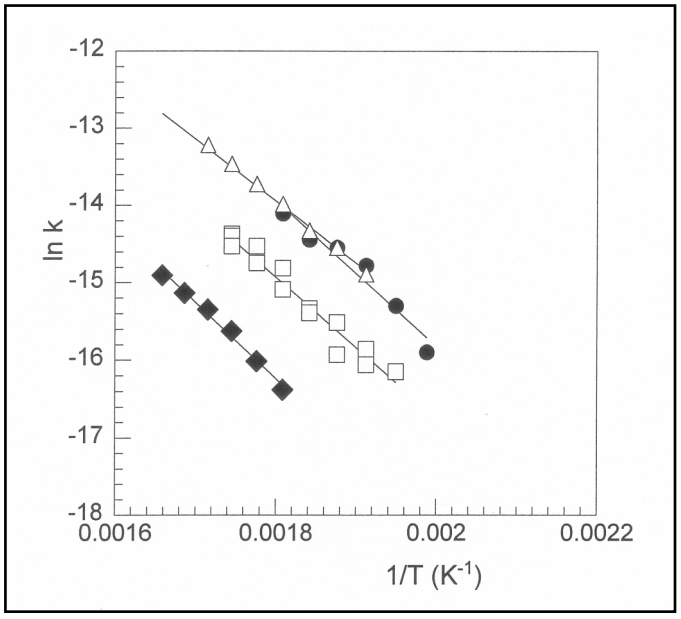

Figure 6. Arrhenius plots of CO oxidation for ZVx,y samples.
◆- ZV1.2,2.7; □- ZV2.7,10; △, ZV7.4,2.7; ● ZV22.4,2.7

Finally we try to rationalize the catalytic behavior of the ZVx,y samples in terms of surface species. In the as prepared samples, polymeric V species grow in number and in size at the increase of the V loading. Contemporarily, V_2O_5-like species (polymeric species with a high degree of

condensation) and eventually V_2O_5 crystals form at V content increase. The vanadium of both V_2O_5-like species and crystalline V_2O_5 can diffuse into the ZrO_2 surface and this process ultimately leads to segregation of ZrV_2O_7. Our results suggest that all these species are active in the CO oxidation and their contribution to the activity chiefly depend on their surface area. In this respect, the major role should be played by the polymeric V species that are the more disperse species, whereas V_2O_5 and ZrV_2O_7 are expected to be present as large particles exposing a little fraction of their vanadium ions.

The leaching with ammonia would dramatically change the surface of the ZVx,y samples as it removes V_2O_5 and the layers of polymeric species not directly interacting with the support, leaving a surface rich of species exposing Zr-O-V bonds. These species would be the ones that catalyze the CO oxidation less efficiently (higher apparent activation energy) but with an increased preesponential factor k_0.

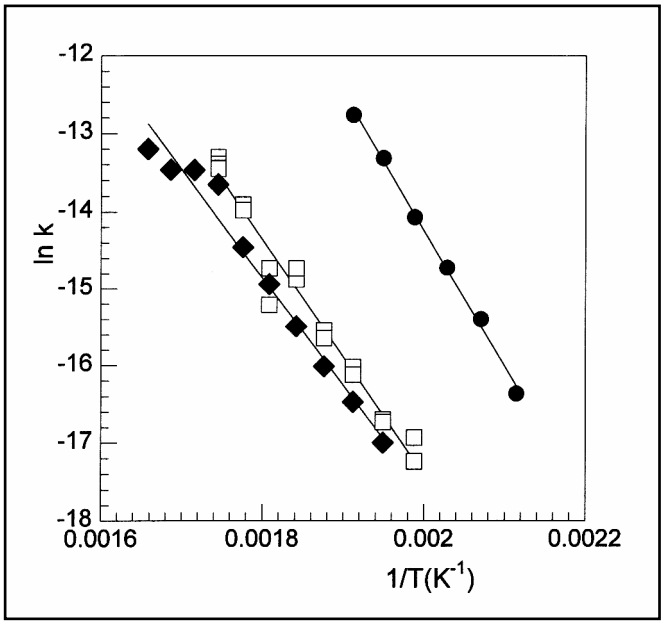

Figure 7. Arrhenius plots of CO oxidation for ZVx,yLz samples.
◆- ZV1.2,2.7L1.1; □- ZV2.7,10L1.4; △- ZV22.4,2.7L7.9.

Conclusions

- The findings for bulk and surface characterization of VO*x*/ZrO_2 catalysts, heated at 823 K in air, show that vanadium is present partly in a dispersed form and partly as ZrV_2O_7 or V_2O_5 or both.

- Raman and TPR data suggest that the dispersed vanadium species are mainly polyvanadate structures and that, after leaching, the fraction of vanadium directly anchored on the zirconia surface is constituted by small polymeric species and ZrV_2O_7 entities.

- All exposed V-containing species are active in the carbon monoxide oxidation. In the as prepared samples polyvanadates are mainly responsible for the activity, as they possess a higher surface area in comparison with V_2O_5 and ZrV_2O_7 large particles.

- Leaching with ammonia exposes a number of species containing Zr-V-O bonds. These sites catalyze the CO oxidation less efficiently (higher E_a), but with a higher pre-exponential factor.

- The large increase in the pre-exponential factor suggests a significant change in the activation entropy of the reaction.

Acknowledgments. Financial support from Italian MIUR (PRIN, Progetti di ricerca di rilevante interesse nazionale) is gratefully acknowledged.

References

[1] B. M. Weckhuysen, D. E. Keller, *Catal. Today*, **2003**, *78*, 25.

[2] H. H. Kung*, Adv. Catal*., **1994**, *40*, 1.

[3] F. Cavani, F. Trifirò, *Catal. Today*, **1999**, *51*, 561.

[4] E. A. Memedov, V. Còrtes Corberàn, *Appl. Catal. A*, **1995**, *127,* 1.

[5] T. Blasco, J.M. L. Nieto, *Appl. Catal. A*, **1997**, *157*, 117.

[6] A. A. Lemonidou, L. Nalbandian, I.A. Vasalos, *Catal. Today*, **2000**, *61*, 333.

[7] F. Roozeboom, A. Jos van Dillen J. W. Geus, P. J. Gellings*, Ind. Eng. Chem. Prod. Res. Dev*. **1981**, *20*, 304.

[8] K. Mori, A. Miyamoto, Y. Murakami, *J. Phys. Chem*., **1984**, *88*, 2735.

[9] M. Ruitenbeek, A. J. van Dillen, F. M. F. de Groot, I. E. Wachs, J. W. Geus, D. C. Koningsberger, *Top. Catal.*, **2000**, *10*, 241.

[10] P. R. Shah, M. M. Khader, J. M. Vohs, R. J. Gorte, *J. Phys. Chem. C***, 2008,** *112*, 2613.

[11] M. Valigi, D. Gazzoli, G. Ferraris and E. Bemporad, *Phys. Chem. Chem. Phys.*, **2003**, *5*, 4974.

[12] M. Valigi, D. Gazzoli , G. Ferraris, S. De Rossi and R. Spinicci, *J. Mol. Catal. A: Chemical*, **2005**, *227,* 59.

[13] M. Valigi, D. Gazzoli, G. Ferraris, S. De Rossi, L. Ferrari, S. Selci, *Appl. Surf. Sci.,* **2008**, *255*, 2012.

[14] D. Gazzoli, S. De Rossi, G. Ferraris, G. Mattei, R. Spinicci and M. Valigi, *J. Molec. Catal. A***: 2009.** doi:10.1016/j.molcata.2009.05.014.

[15] A. Cimino, S. De Rossi, R. Dragone, G. Ferraris, D. Gazzoli, M. Valigi, *J. Colloid Interf. Sci.*, **1998**, *201*, 278.

[16] M. Sanati, A. Andersson, L.R. Wallenberg, B. Rebenstorf, *Appl. Catal*., **1993**, *106*, 51.

[17] R. C. Weast, M. J. Astle (Eds.), C.R.C. Handbook of Chemistry and Physics, 63rd ed., C. R. C. press, Inc. Boca Raton, Florida, **1982**, p. B–162.

[18] P. E. Thomas and W. F. Pickering, *Talanta,* **1971,** *18*, 127 .

[19] I. Pettiti, D. Gazzoli, M. Inversi, M. Valigi, S. De Rossi, G. Ferraris, P. Porta, S. Colonna, *J. Synchr. Rad*., **1999**, *6,* 1120.

[20] S. De Rossi, G. Ferraris, M. Valigi, D. Gazzoli*, Appl. Catal. A: Gen*., **2002**, *231,* 173.

[21] G. A. Parks, *Chem. Rev*., **1965**, *65*, 177 .

[22] Chuah, S. Jaenicke and B. K. Pong, *J. Catal*., **1998**, *175*, 80.

[23] M. T. Pope, in Heteropoly and Isopoly Oxometallates, Springer-Verlag, Berlin, 1983, pp. 1–179.

[24] R. J. Clark, in Comprehensive Inorganic Chemistry, eds. J. C. Bailar, H. J. Emeleus, R. Nyholm and A. F. Trotman-Dickerson, Pergamon Press, Oxford, 1973, vol. 3, pp. 491–551.

[25] M. Valigi, D. Gazzoli, A. Cimino and E. Proverbio, *J. Phys. Chem*., **1999**, *103*,11318.

[26] I. E. Wachs*, Catal. Today*, **1996**, *27*, 437.

[27] A. Khodakov, B. Olthof, A. T. Bell and E. Iglesia, *J. Catal*., **1999**, *181*, 205.

[28] X. Gao, J. Jehng and I. E. Wachs, *J. Catal*., **2002**, *209*, 43.

[29] A. Christodoulakis, M. Machli, A.A. Lemonidou, S. Boghosian, *J. Catal*., **2004**, *222,* 293.

[30] D.E. Keller, D.C. Koningsberger, B.M. Weckhuysen, *J. Phys. Chem. B*, **2006**, *110* (,14313.

[31] J. Pieck, S. del Val, M. L. Granados, M.A. Bañares and J.L.G. Fierro, *Langmuir*, **2002**, *18*, 2642 .

[32] F. Roozeboom, M.C. Mittelmeijer-Hazeleger, J.A. Moulijn, J. Medema, V.H.J. de Beer, P.J. Gellings, *J. Phys. Chem*., **1980**, *84*, 2783.

[33] A. Adamski, Z. Sojka, K. Dyrek, M. Che, G. Wendt and S. Albrecht, *Langmuir* **1999**, *15*, 5733.

[34] G. Deo and I.E. Wachs, *J. Catal*., **1991**, *129*, 307.

[35] T. S. Evans J.C. Hanson A.W. Sleight, *Acta Crystall. B,* **1998**, *54*, 705.